

An elastic-viscoplastic model for saturated frozen soils

S. A. Ghoreishian Amiri^{*}, G. Grimstad, M. Kadivar

Norwegian University of Science and Technology (NTNU), Trondheim, Norway

Abstract

From the material science point of view, saturated frozen soil is a natural particulate composite, composed of solid grains, ice and unfrozen water. The mechanical behavior of such a material is strongly affected by the amount of ice. The amount of ice depends on the temperature and the applied mechanical stresses. The influence of ice content and temperature on the mechanical behavior and the coupling effects on the reverse direction can be mentioned as the main difference between frozen and unfrozen soils. On the other hand, considering the highly rate dependent behavior of ice, rate sensitive behavior of frozen soils is expected. This rate dependency is also affected by the amount of ice existed in the composite. In the light of these differences, an elastic-viscoplastic constitutive model for describing the mechanical behavior of saturated frozen soils is proposed. By dividing the total stress into fluid pressure and solid phase stress, in addition to consideration of the cryogenic suction, the model is formulated within the framework of two-stress state variables. The rate dependent behavior is considered by using the so called over-stress method. In unfrozen state, the model becomes a conventional elastic-viscoplastic critical state model. Model predictions are compared with the available test results and reasonable agreement is achieved.

Keywords: Frozen soil, Constitutive model, Rate effect, Cryogenic suction, Solid-phase stress

^{*} Corresponding author
E-mail address: seyed.amiri@ntnu.no

1 Introduction

The first step in developing a constitutive model for a composite material like frozen soil is to identifying the relevant stress state variables. Total stress based models have been widely used in the literature to describe the mechanical behavior of frozen soils (He et al., 2000; Arenson and Springman, 2005; Lai et al., 2008; Lai et al., 2009; Yuanming et al., 2010; Zhu et al., 2010; Xu, 2014). This approach can successfully simulate the behavior due to external mechanical loads. However, they are not able to simulate the deformations under the variation of ice content and/or temperature during a freezing or thawing period. Moreover, working with total stress, description of soil behavior in the presence of unfrozen water will face some significant difficulties which are not clearly addressed.

Effective stress based models by means of total stress minus pore pressure is also proposed by some researchers (Nixon, 1991; Li et al., 2008; Nicolsky et al., 2008; Thomas et al., 2009). In this method, ice phase is actually considered as another fluid phase and its shear strength does not consider in the model. This approach is pragmatically appropriate for simulating ice segregation phenomenon during a freezing period, but soil strength after ice segregation can be mentioned as the main shortcoming of the method.

Considering the analogy between the physics of frozen-saturated and unfrozen-unsaturated soils, Nishimura et al. (2009) proposed a two stress variables constitutive model for simulating the behavior of saturated frozen soils by employing the net stress (i.e. the excess of total stress over ice pressure) and the cryogenic suction as the relevant stress variables. In this method, although the shear strength of ice phase is not explicitly considered in the formulation, but its effect is partly taken into account by increasing the size of the yield surface with increasing cryogenic suction (i.e. reducing temperature). However, this approach is not fully consistent with the actual microscopic description of the freezing process. According to Wettlaufer and Worster (2006), there exists two types of mechanisms that control the behavior regarding ice content and temperature variations: curvature-induced premelting and interfacial premelting mechanisms. The former is the result of surface tension and acts very similar to the capillary suction by bonding the grains together. Whereas the latter is the result of disjoining pressure (as a repelling force between ice and solid

grains) and tends to widen the gap by sucking in more water. In the model proposed by Nishimura et al. (2009), curvature-induced premelting mechanism is effectively considered by noting the analogy between the capillary and cryogenic suctions, but the interfacial premelting mechanism, which is the main difference of the effects of capillary and cryogenic suctions, is not taken into account. By missing this effect, for simulating a freezing period in this model, ice pressure increases and finally results in zero or negative values of net mean stress, and is followed by a tensile failure and soil particles segregation. According to this approach, samples which have experienced a tensile failure (due to segregation phenomenon) by decreasing temperature under isotropic stress condition, will always show dilative behavior upon shearing. More recently, Zhang and Michalowski (2015) proposed another approach by introducing the effective stress (i.e. total stress minus water pressure) and the pore ice ratio (i.e. the ratio of the volume of ice on the volume of solid particles) as the independent variables for their constitutive model. This kind of effective stress would create an unrealistically high effective confining pressure, if the unfrozen water content approaches zero. The frost heave phenomenon, in this model, is simulated using a porosity growth function. Ghoreishian Amiri et al. (2016) proposed another two stress variables model by introducing the solid phase stress and the cryogenic suction as the relevant stress variables. The solid phase stress is defined as the combined stress in the soil grains and ice. Thus the contribution of the ice phase in carrying the shear stress of the system is implicitly considered in the model. In this model, the curvature-induced premelting mechanism is taken into account in a way similar to that proposed by Nishimura et al. (2009). But the ice segregation phenomenon is simulated by introducing another yield criterion due to suction variation. This approach is consistent with the interfacial premelting mechanism.

In this study, the above mentioned elastic-plastic model (Ghoreishian Amiri et al., 2016) is extended to an elastic-viscoplastic version. The model is developed based on the overstress framework which is originally proposed by Perzyna (1966) and followed by many researchers in the field of geotechnical engineering [e.g. (Grimstad et al., 2010; Yin and Tong, 2011; Yin et al., 2011)].

Note that throughout this paper, compressive stress and strain are assumed to be positive.

2 Model Formulation

Following the discussion presented in Ghoreishian Amiri et al. (2016), the solid phase stress and the cryogenic suction are considered as the relevant stress variables:

$$\boldsymbol{\sigma}^* = \boldsymbol{\sigma} - s_w p_w \mathbf{I} \quad (1)$$

$$S = p_i - p_w = -\rho_i l \ln \frac{T}{T_0} \quad (2)$$

where $\boldsymbol{\sigma}^*$ is the solid phase stress, s_w is the unfrozen water saturation (i.e. the ratio of the volume of unfrozen water on the volume of frozen and unfrozen water), \mathbf{I} denotes the unit tensor, S is the cryogenic suction, p_w and p_i denote the pressure of water and ice phases, respectively, ρ_i indicates the density of ice, l is the specific latent heat of fusion, T stands for temperature on the thermodynamic scale and T_0 is the freezing/thawing temperature of water/ice at a given pressure.

Similar to the reference elastic-plastic model (Ghoreishian Amiri et al., 2016), any strain increment is decomposed into two major parts due to variations of solid phase stress and suction. In this model, elastic-viscoplastic behavior is considered for the deformation due to variation of solid phase stress, while elastic-plastic behavior is assumed for the suction induced deformation. Thus, any strain increment, $d\boldsymbol{\varepsilon}$, can be additively decomposed into the following parts

$$d\boldsymbol{\varepsilon} = d\boldsymbol{\varepsilon}^{me} + d\boldsymbol{\varepsilon}^{se} + d\boldsymbol{\varepsilon}^{mvp} + d\boldsymbol{\varepsilon}^{sp} \quad (3)$$

where $d\boldsymbol{\varepsilon}^{me}$ and $d\boldsymbol{\varepsilon}^{mvp}$ are the elastic and viscoplastic parts of the strain due to the solid phase stress variation, $d\boldsymbol{\varepsilon}^{se}$ and $d\boldsymbol{\varepsilon}^{sp}$ are the elastic and plastic parts of the strain due to the cryogenic suction variation, respectively.

2.1 Elastic Response

The elastic part of the strain due to the solid phase stress variation can be calculated based on the equivalent elastic parameters of the mixture

$$\varepsilon_{ij} = \frac{1}{2G} \sigma_{ij} - \frac{3K-2G}{18KG} \sigma_{kk} \delta_{ij} \quad (4)$$

where δ_{ij} the Kronecker's delta, G and K are the equivalent shear modulus and bulk modulus of the mixture, respectively:

$$G = (1 - s_i)G_0 + \frac{s_i E_f}{2(1 + \nu_f)} \quad (5)$$

$$K = (1 - s_i) \frac{(1 + e)p^*}{\kappa_0} + \frac{s_i E_f}{3(1 - 2\nu_f)} \quad (6)$$

where G and K are the equivalent shear modulus and bulk modulus of the mixture, respectively, G_0 and κ_0 stand for the shear modulus and the elastic compressibility coefficient of the soil in an unfrozen state, respectively, p^* is the solid phase mean stress, E_f and ν_f denote the Young's modulus and Poisson's ratio of the soil in the fully frozen state, respectively, and s_i is the ice saturation. Considering the temperature-dependent behavior of ice, the following expression is employed for E_f

$$E_f = E_{f_{ref}} - E_{f_{inc}} (T - T_{ref}) \quad (7)$$

where $E_{f_{ref}}$ is the value of E_f at the reference temperature (T_{ref}) and $E_{f_{inc}}$ denotes the rate of change in E_f with temperature.

The elastic part of the strain due to suction variation is calculated as

$$d\mathbf{\varepsilon}^{se} = \frac{\kappa_s}{3(1 + e)} \times \frac{dS}{(S + p_{at})} \mathbf{I} \quad (8)$$

where κ_s is the compressibility coefficient due to suction variation within the elastic region, e is the void ratio and p_{at} is the atmospheric pressure.

2.2 Reference, Dynamic and Yield Surfaces

As mentioned earlier, the elastic-viscoplastic model is developed based on the overstress framework (Perzyna, 1966) and the elastic-plastic model presented by Ghoreishian Amiri et al. (2016). In the overstress method, instead of the common yield surface, reference and dynamic surfaces should be defined. Then, the inelastic deformation can be calculated based on the distance of the reference and dynamic surfaces.

For consistency, when the value of cryogenic suction becomes zero, the model should reduce to a common unfrozen soil model. In accordance with the aim of simplicity, the simple elastic-viscoplastic Cam-clay based model is adopted for the unfrozen state. For frozen states, a suction-dependent yield surface for the reference strain rate is required to capture the curvature-induced premelting effects. This surface is recognized as the Loading Collapse (LC) reference surface:

$$F_r = \left[p_r^* - \left(\frac{p_{yr}^* + p_{tr}^*}{2} \right) \right]^2 + \left(\frac{q_r^*}{M} \right)^2 - \left(\frac{p_{yr}^* - p_{tr}^*}{2} \right)^2 = 0 \quad (9)$$

where

$$p_r^* = \frac{(\sigma_r^*)_{11} + (\sigma_r^*)_{22} + (\sigma_r^*)_{33}}{3} \quad (10)$$

$$q_r^* = \sqrt{0.5 \left[((\sigma_r^*)_{11} - (\sigma_r^*)_{22})^2 + ((\sigma_r^*)_{11} - (\sigma_r^*)_{33})^2 + ((\sigma_r^*)_{33} - (\sigma_r^*)_{22})^2 + 3((\tau_r)_{12}^2 + (\tau_r)_{13}^2 + (\tau_r)_{23}^2) \right]} \quad (11)$$

$$p_{yr}^* = p_c^* \left(\frac{p_{y0r}^*}{p_c^*} \right)^{\frac{\lambda_0 - \kappa}{\lambda - \kappa}} \quad (12)$$

$$\lambda = \lambda_0 [(1 - r) \exp(-\beta S) + r] \quad (13)$$

and σ_r^* indicates a stress point on the LC reference surface, M stands for the slope of the critical state line, p_{tr}^* shows the apparent cohesion of the soil, p_c^* indicates the reference stress, p_{y0r}^* is the reference preconsolidation stress for unfrozen condition, κ denotes the compressibility coefficient of the system

within the elastic region ($\kappa = \frac{1+e}{K} p^*$), λ_0 represents the compressibility coefficient for the unfrozen state along virgin loading, r is a constant related to the maximum stiffness of the soil (for infinite cryogenic suction) and β is a parameter controlling the rate of change in soil stiffness with suction. It should be noted, the selected LC reference surface has been previously adopted as a yield surface by Nishimura et al. (2009) for elastic-plastic modelling of frozen soil behavior. However, it has been originally introduced by Alonso et al. (1990) for unsaturated soils.

The LC dynamic surface should always pass through the current stress state (p^*, q^*, S) and also keep a similar shape to the LC reference surface with respect to a similarity line (or the corresponding similarity center in the $p^* - q^*$ space). In this model, the line $S = 0$ is considered as the similarity line. This results in the following geometrical properties:

1. All lines connecting an arbitrary point like (p^*, q^*, S) on the LC dynamic surface and its conjugated point on the LC reference surface join at the $(0, 0, S)$.
2. All ratios of the distance of any arbitrary point like (p^*, q^*, S) on the LC dynamic surface from the similarity center, $(0, 0, S)$, to the distance of its conjugated point on the LC reference surface from the similarity center, $(0, 0, S)$, are identical. This ratio is called the similarity ratio, R , and coincides with the ratio of the sizes of these surfaces.

The LC dynamic surface is described as

$$F_d = \left[p^* - \left(\frac{p_{yd}^* + p_{td}^*}{2} \right) \right]^2 + \left(\frac{q^*}{M} \right)^2 - \left(\frac{p_{yd}^* - p_{td}^*}{2} \right)^2 = 0 \quad (14)$$

where

$$p_{yd}^* = R \cdot p_{yr}^* \quad (15)$$

$$p_{td}^* = R \cdot p_{tr}^* \quad (16)$$

p^* and q^* are the solid phase mean stress and deviatoric stress, respectively, and R indicates the similarity ratio of LC dynamic and LC reference surfaces.

On the other hand, due to the interfacial premelting mechanism, increase of cryogenic suction could lead to grain segregation. As mentioned earlier, this phenomenon is considered with an elastic-plastic behavior and the Grain Segregation (GS) yield criterion is adopted as

$$F = S - S_{seg} = 0. \quad (17)$$

where S_{seg} is the threshold value of suction for ice segregation phenomenon. Figure 1 shows the reference, dynamic and yield surfaces of the model in $p^* - S$ and $p^* - q^*$ planes.

2.3 Hardening Rules

A plastic compression due to the variation of solid phase stress results in stiffer behavior of the soil and causes the LC reference surface to move outward. Furthermore, this plastic compression results in a decrease in the dimensions of voids, hence, lower segregation threshold value is expected. This behavior could be captured by a coupled hardening rule, which causes the GS yield surface to shift downward. Figure 2 shows a typical evolution of LC reference and GS yield surfaces due to a plastic compression in $p^* - S$ and $p^* - q^*$ planes.

A plastic dilation due to occurrence of ice segregation causes the GS yield surface to move upward. This plastic dilation results in softer behavior of the soil, hence, an inward movement of the LC reference surface should also be considered (figure 3).

The above mentioned changes in the LC reference and GS yield surfaces can be represented in the model by the following hardening rules

$$\frac{dp_{y_{0r}}^*}{p_{y_{0r}}^*} = \frac{1+e}{\lambda_0 - \kappa_0} d\varepsilon_v^{mvp} + \frac{1+e}{\lambda_0 - \kappa_0} d\varepsilon_v^{sp} \quad (18)$$

$$\frac{dS_{seg}}{S_{seg} + p_{at}} = -\frac{1+e}{s_w(\lambda_s + \kappa_s)} d\varepsilon_v^{sp} - \frac{1+e}{(\lambda_s + \kappa_s)} \left(1 - \frac{S}{S_{seg}}\right) d\varepsilon_v^{mvp} \quad (19)$$

where λ_s is the compressibility coefficient for an increase in suction across the virgin state. The evolution of the GS yield surface in equation (19) depends on the value of unfrozen water saturation. Actually, the amount of plastic strain due to increase of cryogenic suction (interfacial premelting mechanism) depends on the availability of water. The lower unfrozen water saturation of a freezing fringe, the lower permeability for water to be sucked in. So, the suction-induced strain becomes smaller and smaller. In other words, plastic resistance of the soil, which is the result of the hardening rule, increases by decreasing water saturation.

In addition, as stated by Arenson et al. (2004), Yamamoto and Springman (2014) and Xie et al. (2014), the bonds between soil grains and ice will crack by developing shear strain. On the other hand, these bonds will recover and be stronger by increasing suction. Thus, the following hardening rule is suggest for p_{ir}^*

$$\frac{dp_{ir}^*}{p_{ir}^*} = -k_{t_1} \frac{dS}{p_{ir}^*} \left(H(-p_{ir}^*) \times H(dS) \right) - k_{t_2} \cdot d\varepsilon_q^{mvp} \quad (20)$$

where k_{t_1} and k_{t_2} are model parameters, and H is the Heaviside function

$$H(x) = \begin{cases} 0 & x \leq 0 \\ 1 & x > 0 \end{cases} \quad (21)$$

Figure 4, shows a typical evolution of the LC reference surface due to plastic shear strain, in $p^* - q^*$ plane.

2.4 Flow Rules

The viscoplastic part of the strain increment due to variation of solid phase stress is calculated with the following flow rule based on the similarity ratio

$$d\varepsilon^{mvp} = \mu \left\langle R^N \right\rangle \frac{\partial Q_1}{\partial \sigma^*} \cdot dt = \Delta \lambda_1 \times \frac{\partial Q_1}{\partial \sigma^*} \quad (22)$$

where, $\langle \rangle$ is the Macaulay brackets, dt is the time increment, μ stands for the fluidity of the system corresponding to the reference strain rate, N is the strain rate coefficient and Q_1 is the plastic potential function

$$Q_1 = \left[p^* - \frac{(1 + \gamma s_i) P_{yd}^* + (1 - \gamma s_i) P_{td}^*}{2} \right]^2 + \left(\frac{q^*}{M} \right)^2 \quad (23)$$

where γ is a material parameter.

In common unfrozen soils, μ and N are considered as constant parameters, while in frozen soils this assumption should be examined more precisely. Thus, we can consider the concept of these parameters in a simple 1D model. In the overstress method, the main idea is to calculate the plastic strain rate for the reference strain rate, $\dot{\epsilon}_v^r$, and then to scale it to the current rate (see figure 4)

$$\dot{\epsilon}_v^{vp} = \dot{\epsilon}_v^r \frac{\lambda - k}{\lambda} \left(\frac{P_{cd}}{P_{cr}} \right)^N = \mu \left(\frac{P_{cd}}{P_{cr}} \right)^N \quad (24)$$

As shown in the figure, assuming constant slopes for the lines in $\epsilon_v - \ln \sigma'_v$ plane (i.e. λ) and in $\ln \dot{\epsilon}_v - \ln \sigma'_v$ plane (i.e. N) for different strain rates is crucial in this concept. On the other hand, the parameter μ actually carries the reference strain rate ($\dot{\epsilon}_v^r$), κ and λ , where all of them are considered to be constant. However, in frozen states, κ and λ is varying with ice content, temperature and cryogenic suction. Thus, we need to transfer the reference curve to the current state of ice content, temperature and suction to be able to scale the plastic strain rate from the reference rate to the current rate (see figure 5). This can simply considered as

$$\dot{\epsilon}_v^{mvp} = \dot{\epsilon}_v^r \frac{\lambda - k}{\lambda} \left(\frac{P_{yd}^*}{P_{yr}^*} \right)^{N_s} = \mu_0 \frac{\lambda_0 (\lambda - k)}{\lambda (\lambda_0 - k_0)} \left(\frac{P_{yd}^*}{P_{yr}^*} \right)^{N_s} \quad (25)$$

where μ_0 is the fluidity of unfrozen soil for the reference strain rate.

On the hand, we know that rate dependency of an unfrozen sample is less than a frozen sample. So, lower value of strain rate coefficient, N , for higher ice content is expected. However, rate dependency of ice decreases with decreasing temperature. Thus, higher value of N for higher suction should be expected. These dependencies of N could be considered as

$$N = N_0 + b_1 \times S - b_2 \times s_i \quad (26)$$

where N_0 is the strain rate coefficient of unfrozen soil, and b_1 and b_2 are two model parameters.

The plastic part of the strain increment due to suction variation is calculated with an associated flow rule

$$d\boldsymbol{\varepsilon}^{sp} = -d\lambda \frac{\partial F}{\partial S} \mathbf{I} \quad (27)$$

where $d\lambda$ is the plastic multiplier regarding to SG yield surface. It is worth reminding that the suction-induced plastic strain (equation 27) is the result of the interfacial premelting mechanism.

3 Determination of The Parameters

The proposed model requires ten parameters for describing the behavior under the variation of solid phase stress (G_0 , κ_0 , $E_{f_{ref}}$, $E_{f_{inc}}$, ν_f , γ , $p_{y_{0r}}^*$, p_c^* , λ_0 and M), three parameters regarding to suction-induced strains (S_{seg} , λ_s and κ_s), four parameters for coupling effects (β , r , k_{i_1} and k_{i_2}) and four parameters for rate effects (μ_0 , N_0 , b_1 and b_2).

Plotting the results of an isotropic drained compression test for an unfrozen state of the soil in $v : \ln p$ plane can provide the data to find the elastic compressibility coefficient, κ_0 , the reference stress, p_c^* , the initial value of the reference preconsolidation stress, $p_{y_{0r}}^*$, and the elasto-plastic compressibility coefficient, λ_0 .

Note that the parameters $p_{y_{0r}}^*$ and p_c^* should be determined with respect to the reference strain rate.

A normal drained shear strength test at an unfrozen state of the soil can be used for determining the elastic shear modulus of the soil in unfrozen state, G_0 , and also for the slope of the critical state line (M).

Conducting an unconfined triaxial compression test in an arbitrary reference temperature at a frozen state of the soil, can be used for determining the reference Young's modulus of the frozen soil, $E_{f,ref}$. Similar test in a different negative temperature can be considered to find $E_{f,inc}$. Then, an isotropic compression test at a frozen state of the soil with a certain value of ice saturation can be used for calculating the Poisson's ratio of the soil in the fully frozen state, ν_f , using equation (6).

Considering equation (13), β and r can be calculated by determining λ at two different frozen states of the soil.

The viscous parameters for the unfrozen state of the soil, μ_0 and N_0 , can be determined in a common way from oedometer tests at a constant strain rate or from a conventional oedometer test. Evaluating N in two different frozen states with certain values of cryogenic suction and ice content will provide required data to find b_1 and b_2 . Then, the parameters γ , k_{t_1} and k_{t_2} can be determined using a trial-and-error procedure to fit the time to failure curves of the soil in two different frozen states. Finally, results of a test involving a freezing-thawing cycle plotted in $v : \ln(S + p_{at})$ plane is required to determine the values of S_{seg} , λ_s and κ_s .

4 Model Results

In order to examine the ability of the model to simulate the behavior of frozen soils in an acceptable way, three different series of tests are simulated and compared with model predictions. In the first set, triaxial compression tests on frozen sand samples at different temperatures are simulated to show the ability of the model for representing the stress-strain and volumetric behavior of the soil at different temperatures with a single set of parameters. In the second one, uniaxial compression tests on Fairbanks silt at different strain rates are used to show the ability of the model for considering the rate effects. At the end, a set of creep tests on frozen sands at different temperatures and stress levels are simulated and compared with experiments.

It should be noted that the model is also able to simulate the ice segregation phenomenon and the strength weakening due to pressure melting. These abilities were examined in the elastic-plastic version of the model (Ghoreishian Amiri et al., 2016), thus in the sake of brevity, they are not represented again in this paper.

4.1 Triaxial Tests at Different Temperatures

Xu (2014) reported a series of triaxial compression tests conducted on frozen sand specimens at initial confining pressure of 1 MPa, constant strain rate of $1.67\text{E-}4 \text{ s}^{-1}$ and different temperatures of -1, -2, -5 and -10° C. Since the values of suction were not reported, for the simulations, the Clausius-Clapeyron equation with $l = 334 \text{ MJ/ton}$ and $\rho_i = 0.9 \text{ ton/m}^3$ is used to evaluate the values of suction at the different temperatures. The obtained corresponding suctions, for the samples at -1, -2, -5 and -10° C, are 1.016, 2.036, 5.118 and 10.326 MPa, respectively. The samples were frozen very quickly, so ice segregation was completely avoided. Considering the nature of sandy soils which cannot keep significant amount of unfrozen water below the freezing temperature, $\sigma = \sigma^*$ is assumed in the simulations. The initial void ratio of 0.4 is considered for the tests. The material parameters that are used to predict the soil behavior are listed in table 1. Figure 6 shows a comparison of test data and model predictions for these tests. As shown in the figure, the model can successfully follow the trend of the behavior.

4.2 Uniaxial Compression Tests at Different Strain Rates

Zhu and Carbee (1984) conducted some uniaxial compression tests on frozen Fairbanks silt. The soil tested has 34.2% of plastic limit and 38.4% of liquid limit. The samples were first reached to the desired density by compressing them in acrylic plastic molds with the dimensions of 70 mm in diameter and 152 mm in length. After the specimens were saturated with a vacuum pump, they were placed into a freezing cabinet and frozen quickly to avoid ice lens during freezing. Four different strain rates of $1.1\text{E-}3$, $1.1 \text{ E-}4$, $1.1\text{E-}5$ and $1.1\text{E-}6 \text{ s}^{-1}$ at -3° C are considered in this section for verification of the model. The initial void ratio of 0.3 is considered for the tests. The material parameters that are used to predict the soil behavior are listed in table 2. Comparative results are presented in figure 8.

4.3 Creep Tests at Different Temperatures And Stress Levels

We proceed to validate the model by simulating the creep tests conducted by Eckardt (1979) at different temperature and stress levels . The samples tested were cohesionless sand with medium grain size $d_{50}=0.4$ mm, initial void ratio of 0.5 and dry density of 1750 kg/m^3 . The samples had the dimensions of 100 mm in diameter and 200 mm in length. The tests were done in a cold room, with capability of adjusting temperature with high accuracy. In the tests, different temperatures (-5 and -15°C) are concerned, depending on which, different creep stress, from lowest 1.0 MPa to highest 8.0 MPa, are also considered. Creep stress on samples from frozen, water saturated medium sand was kept constant through testing at different temperatures. The material parameters that are used to predict the soil behavior are listed in table 3. Comparative results are presented in figure 9.

5 Conclusion

In this paper, a two stress-state elastic-viscoplastic model was proposed for simulating the behavior of frozen soils. The model was developed based on the overstress framework (Perzyna, 1966), and the elastic-plastic model presented by (Ghoreishian Amiri et al., 2016). The cryogenic suction and solid phase stress were selected as the independent stress variables. In unfrozen state, the model becomes a conventional elastic-viscoplastic critical state model. Thus, the model can simulate the behavior from a frozen state to an unfrozen state with a single set of parameters. The model was validated against available results of triaxial, uniaxial and creep tests under different temperatures and pressures.

Acknowledgment

This work is carried out as part of CREEP (Creep of Geomaterials, PIAP-GA-2011-286397) project

supported by the European Community through the programme Marie Curie Industry-Academia

Partnerships and Pathways (IAPP) under the 7th Framework Programme, SMACoT (Sustainable Arctic

Marine and Coastal Technology) project supported by the Research Council of Norway through the Centre

for Research based Innovation and IS-TOPP (245997) project supported by the Research Council of

Norway.

REFERENCES

- Alonso, E. E., Gens, A., & Josa, A. (1990). A constitutive model for partially saturated soils. *Géotechnique*, 40(3), 405-430.
- Arenson, L. U., Johansen, M. M., & Springman, S. M. (2004). Effects of volumetric ice content and strain rate on shear strength under triaxial conditions for frozen soil samples. *Permafrost and Periglacial Processes*, 15(3), 261-271.
- Arenson, L. U., & Springman, S. M. (2005). Mathematical descriptions for the behaviour of ice-rich frozen soils at temperatures close to 0 °C. *Canadian Geotechnical Journal*, 42(2), 431-442.
- Eckardt, H. (1979). Creep behaviour of frozen soils in uniaxial compression tests. *Engineering Geology*, 13(1), 185-195.
- Ghoreishian Amiri, S. A., Grimstad, G., Kadivar, M., & Nordal, S. (2016). A constitutive model for rate-independent behavior of saturated frozen soils. *Canadian Geotechnical Journal*, 53(10), 1646-1657.
- Grimstad, G., Degago, S. A., Nordal, S., & Karstunen, M. (2010). Modeling creep and rate effects in structured anisotropic soft clays. *Acta Geotechnica*, 5(1), 69-81.
- He, P., Zhu, Y., & Cheng, G. (2000). Constitutive models of frozen soil. *Canadian Geotechnical Journal*, 37(4), 811-816.
- Lai, Y., Jin, L., & Chang, X. (2009). Yield criterion and elasto-plastic damage constitutive model for frozen sandy soil. *International Journal of Plasticity*, 25(6), 1177-1205.
- Lai, Y., Li, S., Qi, J., Gao, Z., & Chang, X. (2008). Strength distributions of warm frozen clay and its stochastic damage constitutive model. *Cold Regions Science and Technology*, 53(2), 200-215.
- Li, N., Chen, F., Xu, B., & Swoboda, G. (2008). Theoretical modeling framework for an unsaturated freezing soil. *Cold Regions Science and Technology*, 54(1), 19-35.
- Nicolsky, D. J., Romanovsky, V. E., Tipenko, G. S., & Walker, D. A. (2008). Modeling biogeophysical interactions in nonsorted circles in the Low Arctic. *Journal of Geophysical Research: Biogeosciences*, 113(G3), G03S05.
- Nishimura, S., Gens, A., Jardine, R. J., & Olivella, S. (2009). THM-coupled finite element analysis of frozen soil: formulation and application. *Géotechnique*, 59(3), 159-171.
- Nixon, J. F. (1991). Discrete ice lens theory for frost heave in soils. *Canadian Geotechnical Journal*, 28(6), 843-859.
- Perzyna, P. (1966). Fundamental Problems in Viscoplasticity. In H. L. D. P. G. L. H. W. O. W. P. R. F. P. G.G. Chernyi & H. Ziegler (Eds.), *Advances in Applied Mechanics* (Vol. 9, pp. 243-377): Elsevier.
- Thomas, H. R., Harris, C., Cleall, P., Kern-Luetschg, M., & Li, Y. C. (2009). Modelling of cryogenic processes in permafrost and seasonally frozen soils. *Géotechnique*, 59(3), 173-184.
- Wettlaufer, J. S., & Worster, M. G. (2006). Premelting dynamics. *Annual Review of Fluid Mechanics*, 38(1), 427-452.
- Xie, Q., Zhu, Z., & Kang, G. (2014). Dynamic stress-strain behavior of frozen soil: Experiments and modeling. *Cold Regions Science and Technology*, 106-107, 153-160.
- Xu, G. (2014). *Hypoplastic constitutive models for frozen soil*. Ph.D Dissertation, University of Natural Resources and Life Sciences, Vienna.
- Yamamoto, Y., & Springman, S. M. (2014). Axial compression stress path tests on artificial frozen soil samples in a triaxial device at temperatures just below 0 °C. *Canadian Geotechnical Journal*, 51(10), 1178-1195.

- Yin, J.-H., & Tong, F. (2011). Constitutive modeling of time-dependent stress–strain behaviour of saturated soils exhibiting both creep and swelling. *Canadian Geotechnical Journal*, 48(12), 1870-1885.
- Yin, Z., Karstunen, M., Chang, C., Koskinen, M., & Lojander, M. (2011). Modeling Time-Dependent Behavior of Soft Sensitive Clay. *Journal of Geotechnical and Geoenvironmental Engineering*, 137(11), 1103-1113.
- Yuanming, L., Yugui, Y., Xiaoxiao, C., & Shuangyang, L. (2010). Strength criterion and elastoplastic constitutive model of frozen silt in generalized plastic mechanics. *International Journal of Plasticity*, 26(10), 1461-1484.
- Zhang, Y., & Michalowski, R. L. (2015). Thermal-Hydro-Mechanical Analysis of Frost Heave and Thaw Settlement. *Journal of Geotechnical and Geoenvironmental Engineering*, 141(7), 04015027.
- Zhu, Y., & Carbee, D. L. (1984). Uniaxial compressive strength of frozen silt under constant deformation rates. *Cold Regions Science and Technology*, 9(1), 3-15.
- Zhu, Z., Ning, J., & Ma, W. (2010). A constitutive model of frozen soil with damage and numerical simulation for the coupled problem. *Science China Physics, Mechanics and Astronomy*, 53(4), 699-711.

Table 1. Model parameters for frozen sand (triaxial tests)

Unfrozen soil shear modulus, MPa	$G_0 = 3.5$
Unfrozen soil elastic compressibility coefficient	$\kappa_0 = 0.08$
Frozen Soil Young's modulus at $T_{ref} = 273.16$ K , MPa	$E_{f_{ref}} = 200$
Rate of change in Young's modulus with temperature, MPa/K	$E_{f_{inc}} = 80$
Frozen Soil Poisson's ratio	$\nu_f = 0.31$
Plastic potential parameter	$\gamma = 0.08$
Initial preconsolidation stress for unfrozen state, MPa	$(p_{y_{0r}}^*)_{in} = 5.55$
Reference stress, MPa	$p_c^* = 0.1$
Elastic-plastic compressibility coefficient for unfrozen state	$\lambda_0 = 0.85$
Slope of the critical state line	$M = 1.5$
Initial segregation threshold, MPa	$(S_{seg})_{in} = 10$
Elastic compressibility coefficient for suction variation	$\kappa_s = 0.008$
Elastic-plastic compressibility coefficient for suction variation	$\lambda_s = 0.4$
Rate of change in apparent cohesion with suction	$k_{t_1} = 0.15$
Hardening parameter for apparent cohesion	$k_{t_2} = 1.5$
Coefficient related to the maximum soil stiffness	$r = 0.66$
Rate of change in soil stiffness with suction, MPa ⁻¹	$\beta = 0.11$
Fluidity parameter for unfrozen state, s ⁻¹	$\mu_0 = 5E - 6$
Rate dependency parameter for unfrozen state	$N_0 = 25$
Rate of change in N with suction, MPa ⁻¹	$b_1 = 0.58$
Rate of change in N with ice saturation	$b_2 = 22$

Table 2. Model parameters for frozen Fairbanks silt

Unfrozen soil shear modulus, MPa	$G_0 = 5$
Unfrozen soil elastic compressibility coefficient	$\kappa_0 = 0.03$
Frozen Soil Young's modulus at $T_{ref} = 273.16$ K , MPa	$E_{f_{ref}} = 140$
Rate of change in Young's modulus with temperature, MPa/K	$E_{f_{inc}} = 10$
Frozen Soil Poisson's ratio	$\nu_f = 0.48$
Plastic potential parameter	$\gamma = 0.01$
Initial preconsolidation stress for unfrozen state, MPa	$(p_{y_{or}}^*)_{in} = 0.9$
Reference stress, MPa	$p_c^* = 0.07$
Elastic-plastic compressibility coefficient for unfrozen state	$\lambda_0 = 0.7$
Slope of the critical state line	$M = 1.05$
Initial segregation threshold, MPa	$(S_{seg})_{in} = 10$
Elastic compressibility coefficient for suction variation	$\kappa_s = 0.008$
Elastic-plastic compressibility coefficient for suction variation	$\lambda_s = 0.4$
Rate of change in apparent cohesion with suction	$k_{t_1} = 0.3$
Hardening parameter for apparent cohesion	$k_{t_2} = 1.5$
Coefficient related to the maximum soil stiffness	$r = 0.49$
Rate of change in soil stiffness with suction, MPa ⁻¹	$\beta = 0.15$
Fluidity parameter for unfrozen state, s ⁻¹	$\mu_0 = 2E - 6$
Rate dependency parameter for unfrozen state	$N_0 = 25$
Rate of change in N with suction, MPa ⁻¹	$b_1 = 0.58$
Rate of change in N with ice saturation	$b_2 = 22$

Table 3. Model parameters for frozen sand (creep tests)

Unfrozen soil shear modulus, MPa	$G_0 = 5$
Unfrozen soil elastic compressibility coefficient	$\kappa_0 = 0.01$
Frozen Soil Young's modulus at $T_{ref} = 273.16$ K , MPa	$E_{f_{ref}} = 140$
Rate of change in Young's modulus with temperature, MPa/K	$E_{f_{inc}} = 10$
Frozen Soil Poisson's ratio	$\nu_f = 0.48$
Plastic potential parameter	$\gamma = 0.01$
Initial preconsolidation stress for unfrozen state, MPa	$(p_{y_{0,r}}^*)_{in} = 0.28$
Reference stress, MPa	$p_c^* = 0.05$
Elastic-plastic compressibility coefficient for unfrozen state	$\lambda_0 = 0.02$
Slope of the critical state line	$M = 0.85$
Initial segregation threshold, MPa	$(S_{seg})_{in} = 10$
Elastic compressibility coefficient for suction variation	$\kappa_s = 0.008$
Elastic-plastic compressibility coefficient for suction variation	$\lambda_s = 0.4$
Rate of change in apparent cohesion with suction	$k_{t_1} = 0.45$
Hardening parameter for apparent cohesion	$k_{t_2} = 2.5$
Coefficient related to the maximum soil stiffness	$r = 0.49$
Rate of change in soil stiffness with suction, MPa ⁻¹	$\beta = 0.15$
Fluidity parameter for unfrozen state, hr ⁻¹	$\mu_0 = 8E - 6$
Rate dependency parameter for unfrozen state	$N_0 = 25$
Rate of change in N with suction, MPa ⁻¹	$b_1 = 0.33$
Rate of change in N with ice saturation	$b_2 = 21.1$

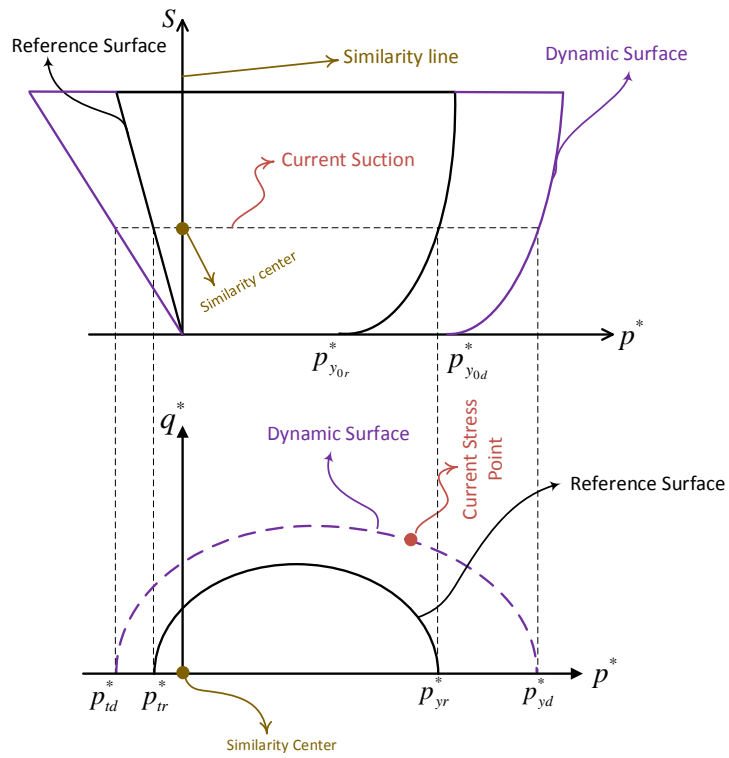


Figure 1. Representation of reference, dynamic and yield surfaces in $p^* - S$ and $p^* - q^*$ planes

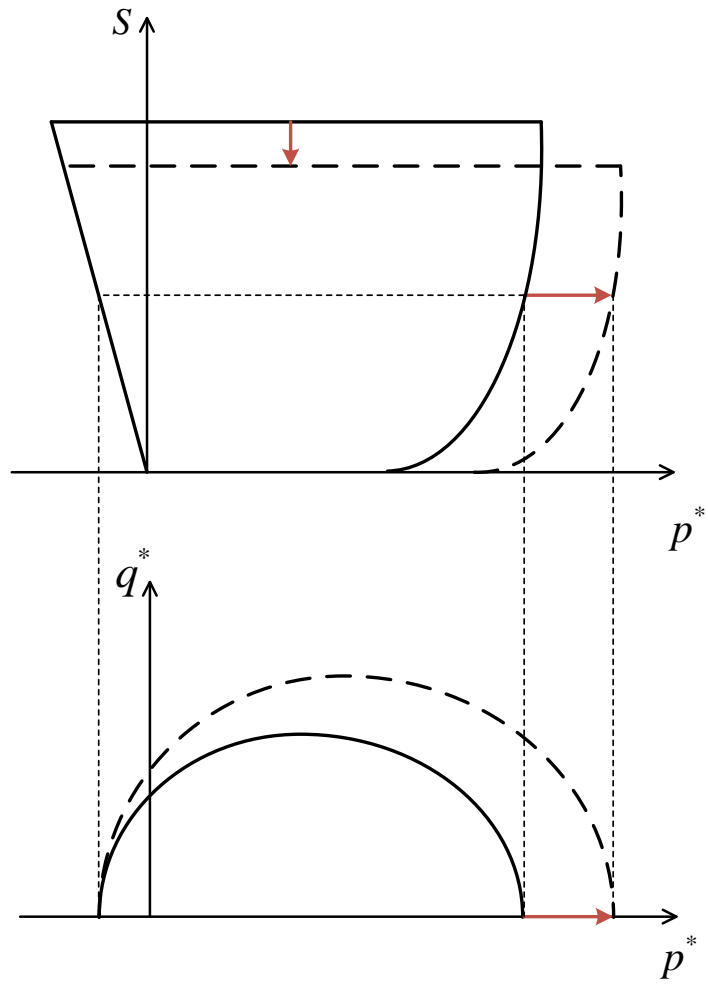


Figure 2. Evolution of LC reference and GS yield surfaces due to plastic compression

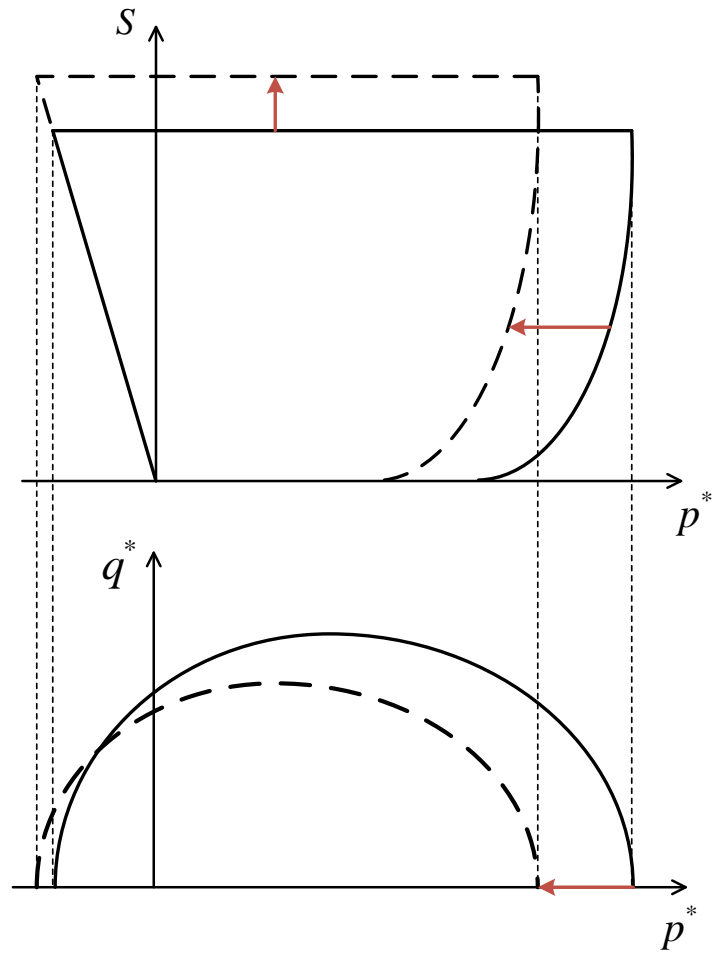


Figure 3. Evolution of LC reference and GS yield surfaces due to ice segregation phenomenon

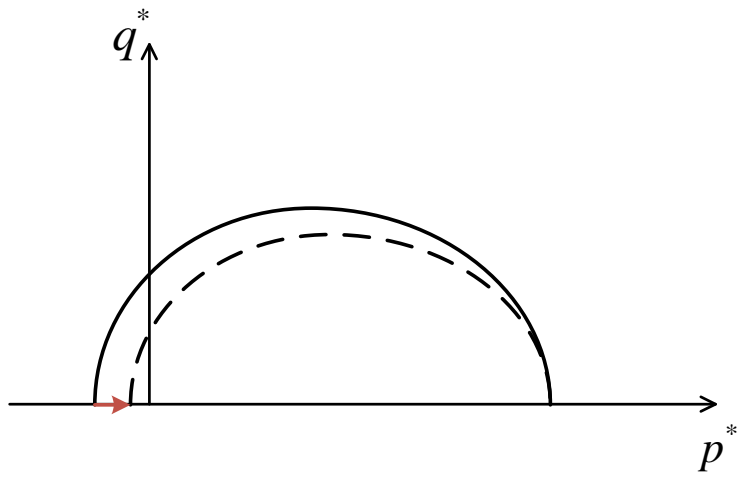


Figure 4. Evolution of LC reference surface in $p^* - q^*$ plane due to plastic shear strain

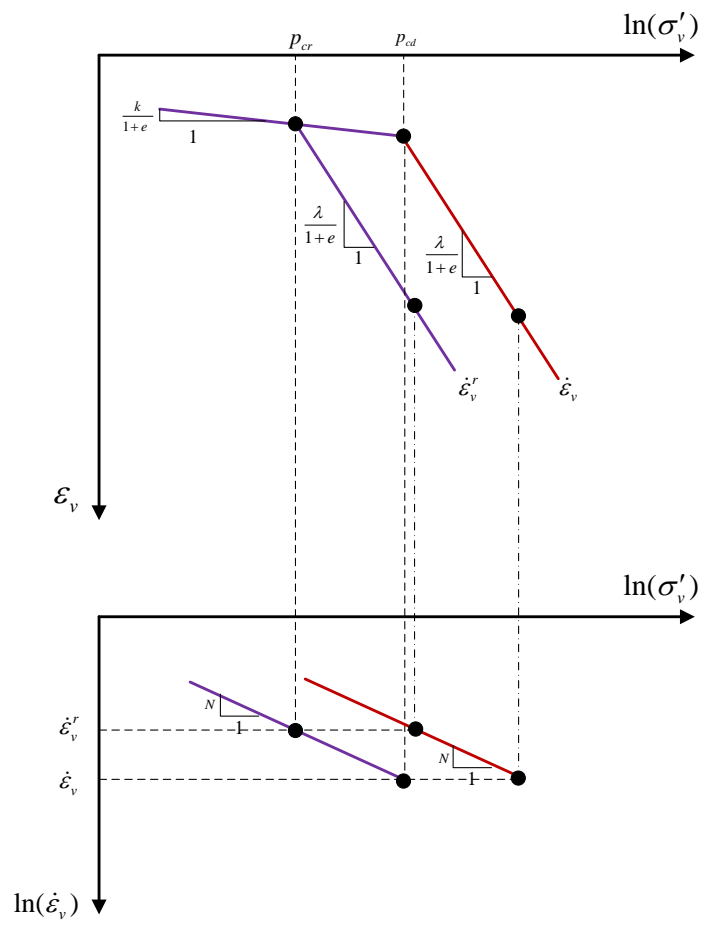


Fig 5. Schematic 1D representation of overstress framework for unfrozen soils

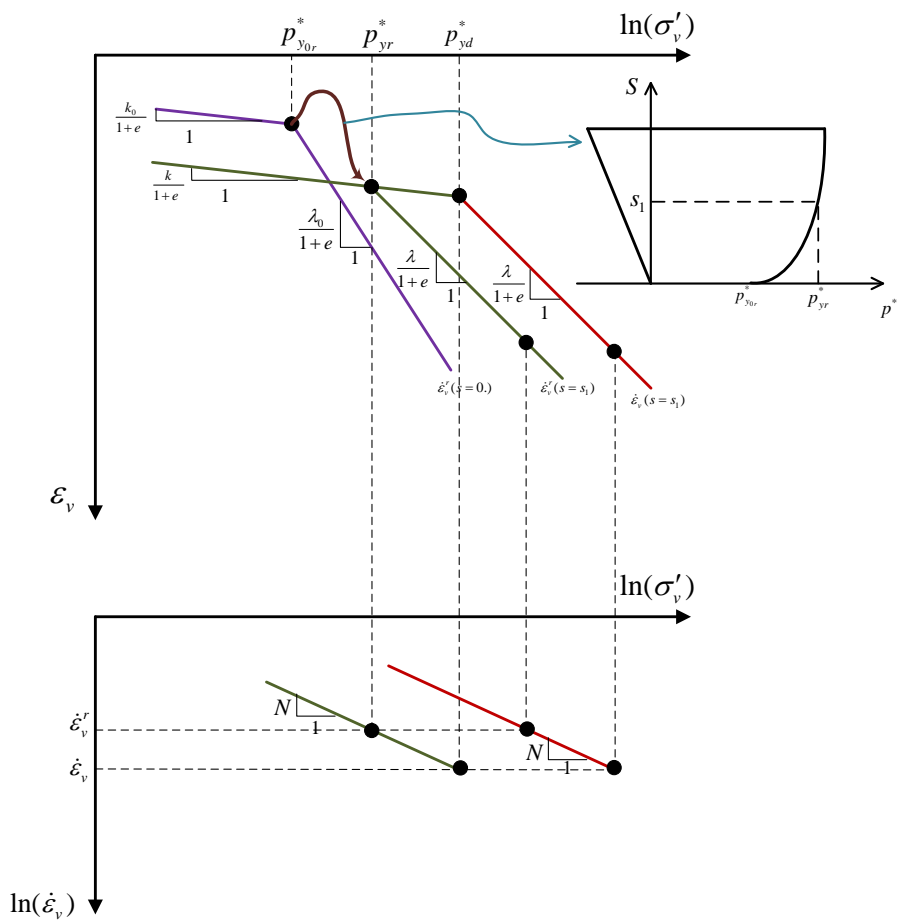


Fig 6. Schematic 1D representation of the overstress framework for frozen soils

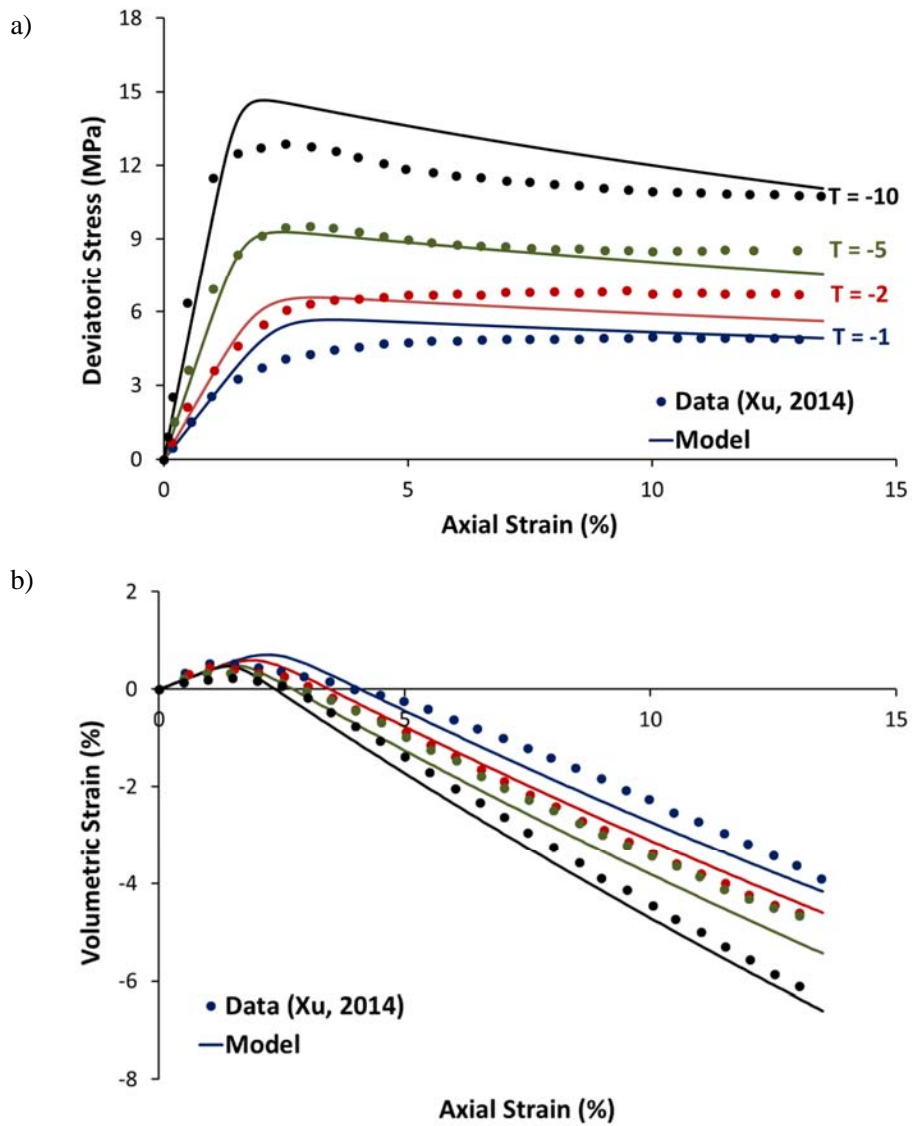


Fig 7. Comparison between the measured and predicted results for triaxial tests under different temperatures: (a) stress-strain relation and (b) volumetric strain

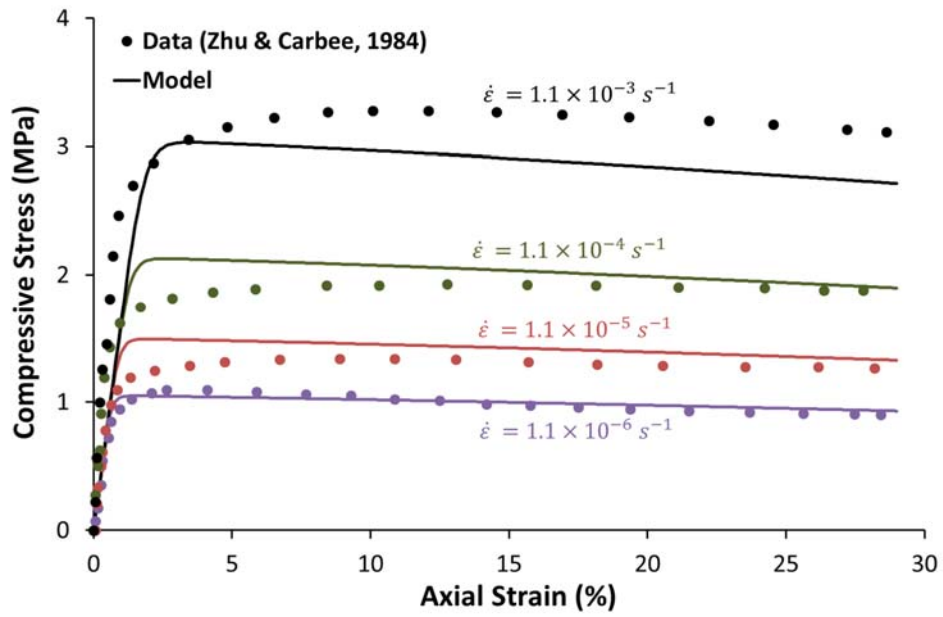


Fig 8. Comparison between the measured and predicted stress-strain curves for frozen Fairbanks silt (-3° C)

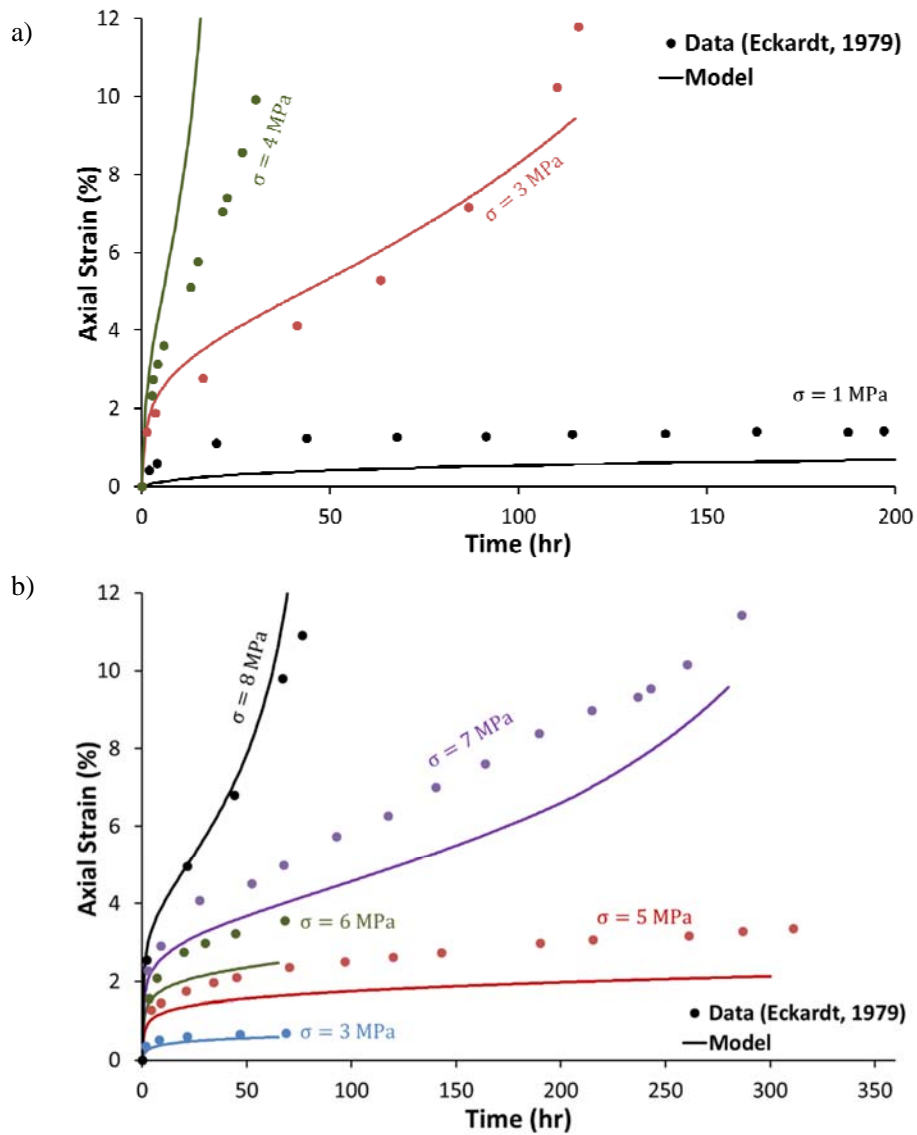


Fig 9. Comparison between the measured and predicted results for uniaxial creep tests at different stress level : (a) at -5°C and (b) at -15°C